Available online at www.sciencedirect.com

ScienceDirect

Procedia Manufacturing 15 (2018) 1062–1070

Procedia MANUFACTURING

www.elsevier.com/locate/procedia

17th International Conference on Metal Forming, Metal Forming 2018, 16-19 September 2018, Toyohashi, Japan

Phase transformations in a boron-alloyed steel at high heating rates

Illia Hordych[a,*], Konrad Bild[a], Viacheslav Boiarkin[b], Dmytro Rodman[a], Florian Nürnberger[a]

[a]*Institut für Werkstoffkunde (Materials Science), Leibniz Universität Hannover, An der Universität 2, Garbsen, 30823, Germany*
[b]*Department of Metal Forming, National Metallurgical Academy of Ukraine, Gagarina av. 4, Dnipro, 49600, Ukraine*

Abstract

Products or semi-finished products featuring tailored properties are highly relevant for many industrial applications. Hence, new technologies that allow to locally adapt mechanical properties are of key interest. For example, tailoring properties in profiles or tubes by a local heat-treatment appear to be promising in combination with subsequent forming operations requiring locally adapted material strength to realize complex shapes. To implement an inline process of tube forming and local heat treatment by inductive heating and spray quenching, dilatometric investigations were carried out for a heat treatable boron-alloyed steel 1.5528 (22MnB5). In particular, focus was on the effect of high inductive heating rates on the austenite formation. The influence of heating rates in the range from 500 K/s to 2500 K/s on the austenitization was evaluated and a continuous time-temperature-austenitization diagram proposed. The results can be used to compute the decomposition of ferrite and pearlite due to inductive heating.

Peer-review under responsibility of the scientific committee of the 17th International Conference on Metal Forming.

Keywords: 22MnB5; Tailored properties; Tube forming; Induction heating; Austenite transformation

* Corresponding author. Tel.: +49-511-762-4313; fax: +49-511-762-5245.
E-mail address: hordych@iw.uni-hannover.de

2351-9789
Peer-review under responsibility of the scientific committee of the 17th International Conference on Metal Forming.
10.1016/j.promfg.2018.07.386

Nomenclature

A_{c1}	start temperature of austenite formation, °C
A_{c3}	finish temperature of austenite formation, °C
T_c	Curie temperature, °C
V_h	heating rate, $K \cdot s^{-1}$
α_{th}	thermal expansion coefficient, K^{-1}
ε_{th}	thermal expansion, %
$\varepsilon_{tr,\alpha\rightarrow\gamma}$	transformation strain of ferrite to austenite, %

1. Introduction

The modern machine industry has been pursuing economic and ecologic products by developing parts adapted to local loadings. Tailored components, including tubes, can be obtained by several methods such as tailoring size and/or properties, combining materials or reinforcing of the most loaded sections locally [1]. Tube forming is widely used to produce welded tubes [2, 3] and represents a suited process to introduce new technologies to tailor properties. The integration of a local heat treatment into a process line is suited for a continuous production when upgrading existing tube forming lines to produce profiles with a constant cross-section.

Using heat treatable boron steels, products featuring a high level of mechanical properties and high wear resistance can be produced [4]. If individual zones of tubes undergo a heat-treatment, alternating ductile and strong sections can be obtained. Tubes featuring tailored properties in the longitudinal direction can be utilized both as finished components as well as semi-finished products for further forming operations. Possible applications of finished products are profiles with a predictable folding or vibration resistance due to a damping effect, e.g. for crash-relevant elements or high-pressure pipelines. Additionally, ductile sections can be exposed to cold post-processing operations such as high-pressure hydroforming, flanging or bending.

2. Tube forming with integrated heat-treatment

The proposed technology consists of a traditional tube forming line in combination with an integrated heat-treatment employed after the welding process (Fig. 1). The tube forming process is usually fulfilled by means of a number of driven multi-roll stands arranged into groups sorted by their purpose (sheet forming, welding, sizing, profile forming) [5]. Sheet forming is carried out by a gradual closing of a metal sheet into a circle. A formed circle is then welded, sized to improve the surface and properties of a recently welded tube and exposed to an inductive heating process with a subsequent air-water spray cooling. The latter methods are advantageous for an inline process due to possible high heating/cooling rates and a contact free impact onto the tube body.

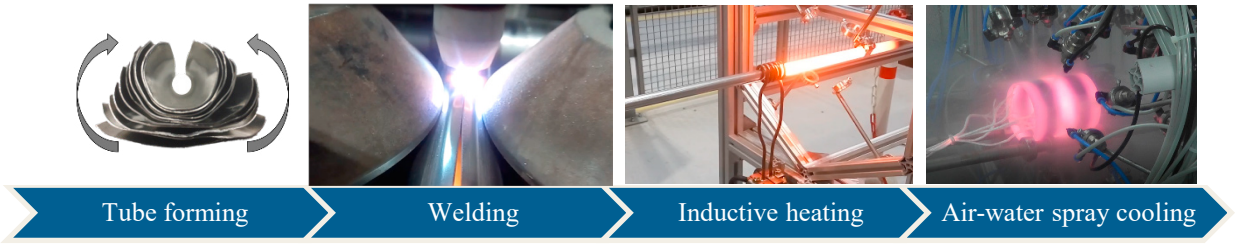

Fig. 1. Layout of tube forming with integrated heat-treatment.

Accordingly, after the last profile forming stand, the tube is rapidly heated up to the austenitizing temperature and immediately quenched by means of an air-water spray. Thus, martensite is formed. A local heat-treatment can be realized, if this procedure is applied to selected areas. The inductive heating should be employed to the whole tube in order to eliminate the work-hardening effect introduced during the forming and to reduce inhomogeneities after

the welding stage. Thus, a selective quenching appears to be preferential for the realization of a local heat-treatment. Spray cooling with a flexible control system allows a precise adjustment of areas to be quenched. Additionally, by employing an air-water spray the cooling rate can be adjusted over a wide range which offers the possibility to generate complex microstructures and hence material properties [6]. The unquenched parts of the tube are cooled by resting air and stay unhardened.

To facilitate the formation of martensite, the microstructure of a certain segment is expected to be fully austenitized. The heating process in a tube forming line limits the available time for heating and soaking. Hence, the steel should be significantly overheated to accelerate diffusive processes of the ferrite-pearlitic decomposition to allow a full austenitizing.

The present study aims to determine the kinetics of the phase transformations during the short-time inductive heating of a boron-alloyed steel. The austenite decomposition during the cooling stage is not in the focus of this work.

3. Methods and materials

The developed technology line is based on a laboratory scale electric pipe-welded profiling machine “Nagel Profiliertechnik 1001” with 13 forming and 3 sizing multi-roll stands for the production of tubes with a diameter of 20 mm and a wall thickness from 0.5 mm to 0.8 mm. The process of tube forming can be carried out with a feed between 0.1 mm/s and 250 mm/s. This wide range is restricted by the welding process. Prior to the first sizing stand, a plasma arc welding station “EWM Microplasma 50” with a maximum current of 50 A is positioned and the preformed tube is joined. This type of welding is beneficial for a continuous production line due to the absence of flash on the internal and external tube surfaces. Pilot investigations revealed that a sufficient welding seam can be obtained at lower feed rates depending on the welding parameters. After the sizing stands, an induction coil of a medium frequency inductor “Eldec MFG 30” with a maximal power of 30 kW is integrated in the process line. Based on the properties and parameters of the welding station as well as of the inductor and considering the geometry of the inductor coil, a necessary minimal heating rate (V_h) can be determined. The length of the induction coil and the feed rate determine the actual heating rate in the first turn. For instance, assuming that the coil has a length of 50 mm at a process rate of 25 mm/s, a steel tube has to be heated to the required temperature within two seconds.

The present study is carried out with the heat treatable boron alloyed steel 1.5528 (22MnB5) fulfilling the requirements of the chemical composition [7] as determined by atomic emission spectroscopy: C – 0.23, Si – 0.30, Mn – 1.23, Cr – 1.16, Ti – 0.04, B – 0.0031, balance Fe, in wt.-%. This steel is mostly applied for press hardening and usually undergoes an oven heating at 900 °C for 3-6 min to be fully austenitized [8].

With the knowledge of the required heating parameters and the available equipment, the range of relevant heating rate was specified between 500 and 2500 K s^{-1}. In [9], the effect of the full hardening using resistance heating was investigated. Nevertheless, such heating parameters for the steel 22MnB5 are not reported in the literature since a heating is usually carried with lower heating rates. E.g., phase transformations of 22MnB5 during heating are described in [10] for heating rates up to 150 K s^{-1} or in [11] for heating rates up to 100 K s^{-1}. The reported rates are significantly lower than the target ones. In order to realize a rapid austenitizing and to observe the phase transformations at these heating rates, dilatometric investigations were carried on a dilatometer DIL 805A/D+T from Bähr. Specimens with the dimensions 10 mm × 5 mm × 1.5 mm were inductively heated with heating rates of 500, 1200, 1800 and 2500 K s^{-1}. Immediately afterwards these were quenched at a cooling rate of 30 K s^{-1}. To compensate the lack of dwell time during inductive heating, the austenitizing temperature was raised up to 1150 °C (above the temperature of formation of the homogeneous austenite at the highest reported heating rate) according to [10]. Three specimens per heating rate were investigated.

The microstructure resulting from the dilatometric investigations was analyzed by optical microscopy. The specimens were mounted, ground and polished down to 1 µm with a diamond paste finish. To contrast the microstructure, the surfaces were etched with 1% HNO_3 for 2 s.

4. Phase transformations during heat treatment

Fig. 2 depicts the measured time-temperature (*t-T*) courses during the dilatometric investigations with different heating rates. The selected results of one sample from three per heating rate are shown for a better visibility. Since the samples were treated at the same parameters, they exhibit low deviations. It can be seen that all of the curves feature two heating intervals with different heating rates. The inflexion point is in the temperature range from 740 °C to 800 °C and rising with an increasing heating rate. This point corresponds to the Curie temperature (T_c), which describes the loss of the material ferromagnetic properties [12]. This phenomenon can be observed at 768 °C for pure iron and at 720 °C - 745 °C for different steel grades [13]. Analyzing the temperature curves it can be seen that the target heating rate are valid up to the T_c. The stepped increase of temperature for the highest heating rates is related to the response time of the dilatometer and should not affect the heating process. After reaching T_c, the actual heating rate decreases and is nearly constant for all experiments with values in the range from 368 K s^{-1} to 380 K s^{-1}. This shows that due to the magnetic properties of the steel it was not possible to obtain higher heating rates with the dilatometric setup employed once the material is paramagnetic. Despite of the decrease of heating rate, these results are important, since they will be accordingly equal in the real process of the inductive heating in the continuous tube forming line. For this technology, an increasing inductor power to hold the given heating rate above the T_c would not be an option due to a possible overheating of the still ferromagnetic sections.

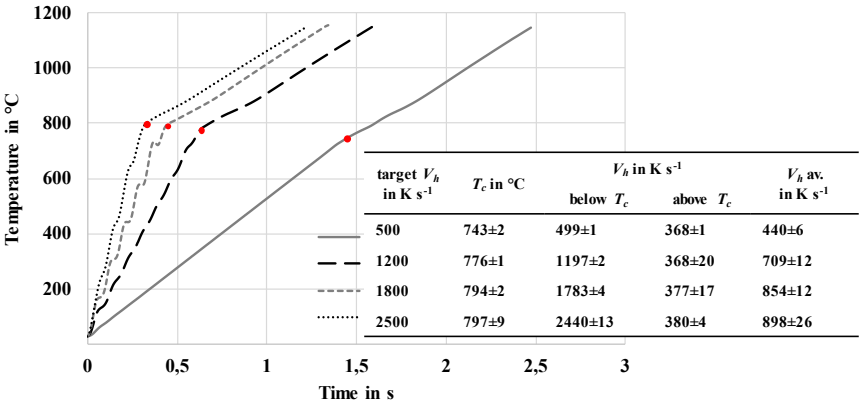

target V_h in K s^{-1}	T_c in °C	V_h in K s^{-1} below T_c	V_h in K s^{-1} above T_c	V_h av. in K s^{-1}
500	743±2	499±1	368±1	440±6
1200	776±1	1197±2	368±20	709±12
1800	794±2	1783±4	377±17	854±12
2500	797±9	2440±13	380±4	898±26

Fig. 2. Time-temperature-course due to inductive heating with corresponding heating rates V_h and marked Curie temperatures T_c.

In the present study, the calculations of the phase transformations during the inductive heating are based on the method described in [14]. The dilatometric curves in the transformation range are depicted in Fig. 3(a). Since the heating rates were relatively equal during the transformation, the dilatometric curves are similar as well. Nevertheless, the displacement of the transformation to higher temperatures with increasing heating rates can be observed. Furthermore, an unusual deviation from the linear course on the ferrite section to higher values of thermal expansion between 750 °C and 830 °C can be noticed. It could be related to the overcoming of the T_c and thus decreasing heating rates.

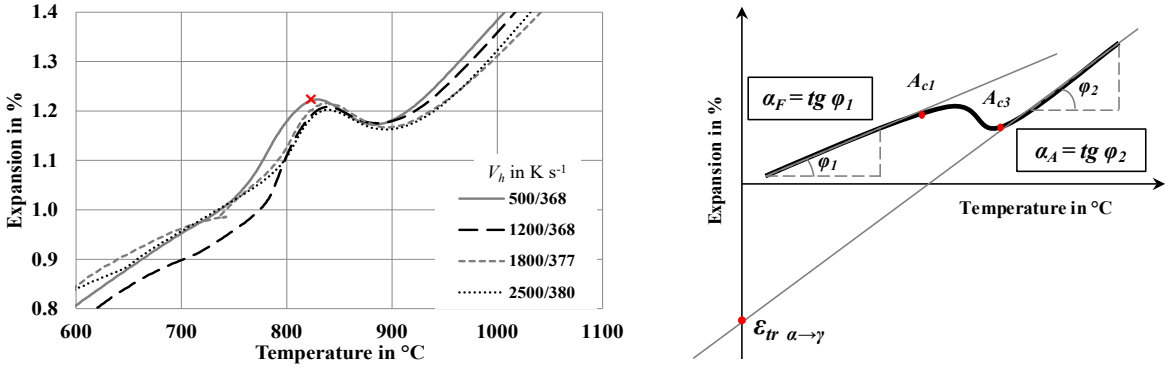

a b

Fig. 3. (a) Dilatometric curves of steel 22MnB5 for different heating rates in K s^{-1} (below/above T_c); (b) schematic representation of determination of data relevant for further calculations.

The A_{c1}- and A_{c3}-temperatures were determined from the dilatometric curves as described in Fig. 3(b). The A_{c1}-temperature indicates the beginning of the transformation and is usually defined as a first point of deviation from a line of the thermal expansion of the ferrite. In the present case, the determination was complicated by the curvature of this line right before the transformation. Thus, the A_{c1}-temperatures were defined as the first points after reaching the highest values of the thermal expansion (exemplary shown in Fig. 3(a) as a red cross). The A_{c1}-temperatures lie in the range from 816 °C to 832 °C with a slight direct dependence on the heating rate. The A_{c3}-temperatures correspond to the finish of transformation and represent the last temperature points before the return to the line of thermal expansion of austenite. Their values cover the range from 946 °C to 995 °C and show a slight dependence on the heating rate as well. Based on these values, a time-temperature-austenitizing diagram with consideration of the investigated heating rates was constructed (Fig. 4). Comparing the experimental data with the literature data published in [10], it can be noticed that the defined start-finish-temperatures increase with increasing heating rates and that they are in good correspondence with the literature data. According to the diagram, an austenitizing temperature of 1000 °C should ensure the austenite formation.

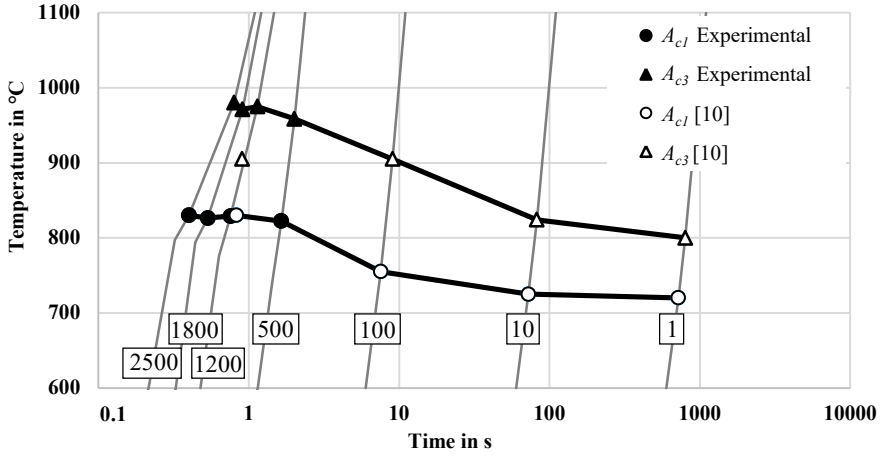

Fig. 4. TTA-diagram of steel 22MnB5, heating rates in K s^{-1} outlined in boxes (literature data according to [10]).

From the dilatometric curves, essential data for the description of the austenite formation can be determined as shown in Fig. 3(b). The change of the thermal expansion during the heating allows the determination of the volume fraction of the present phases. The thermal expansion of ferrite $\varepsilon_{th,F}$ and austenite $\varepsilon_{th,A}$ as well as the transformation strain during the phase transformation of ferrite to austenite $\varepsilon_{tr,\alpha\rightarrow\gamma}$ aggregate to the overall thermal expansion ε_{th} in each point considering the volume fraction f_x of the present phases at a given temperature (Eq. (1)):

$$\varepsilon_{th} = f_F \cdot \varepsilon_{th,F} + f_A \cdot \varepsilon_{th,A} + f_A \cdot \varepsilon_{tr,\alpha\rightarrow\gamma}, \quad (1)$$

where f_A is the volume fraction of austenite and f_F is the volume fraction of ferrite. Knowing that the thermal expansion is a product of the thermal expansion coefficient α_{th} and the material temperature T, Eq. (1) can be presented as:

$$\varepsilon_{th} = f_F \cdot \alpha_{th,F} \cdot T + f_A \cdot \alpha_{th,A} \cdot T + f_A \cdot \varepsilon_{tr,\alpha\rightarrow\gamma}. \quad (2)$$

Assuming that $f_F = 1 - f_A$, the progress of austenite formation can be derived from Eq. (2):

$$f_A(T,t) = \frac{\varepsilon_{th} - \alpha_{th,F} \cdot T(t)}{(\alpha_{th,A} - \alpha_{th,F}) \cdot T(t) + \varepsilon_{tr,\alpha\rightarrow\gamma}}. \quad (3)$$

The $\alpha_{th,F}$ as well as $\alpha_{th,A}$ are obtained from linear sections of the respective phases on the dilatometric curves (as in Fig. 3(b)). The deviation of the ferrite line above the T_c was neglected in this case. With values of $\alpha_{th,F}$ = (14.52±0.17)·10^{-6} K^{-1} for ferrite and $\alpha_{th,A}$ = (23.35±1.11)·10^{-6} K^{-1} for austenite, these correlate adequately with the literature [15]. The $\varepsilon_{tr,\alpha\rightarrow\gamma}$ represents the transformation strain in the extrapolated cross point of the thermal expansion of austenite at the temperature of 0 °C (as in Fig. 3(b)). Since the thermal expansion of austenite is higher than of ferrite, the value of the transformation strain is always negative. For the present investigations, it amounts to -0.99±0.11%.

The volume fraction of austenite from Eq. (3) as a function of the temperature (Fig. 5(a)) as well as of the time (Fig. 5b) show the evolution of austenite formation during the continuous inductive heating. All of the curves represent typical sigmoid curves. The left diagramm confirms the increase of the start-finish-transformation temperatures with increasing heating rates as stated in Fig. 3a. The right diagramm illustrates the absolute difference of the austenite formation in time starting from room temperature and gives information about the required heating time to allow austenitizing at the given heating rates.

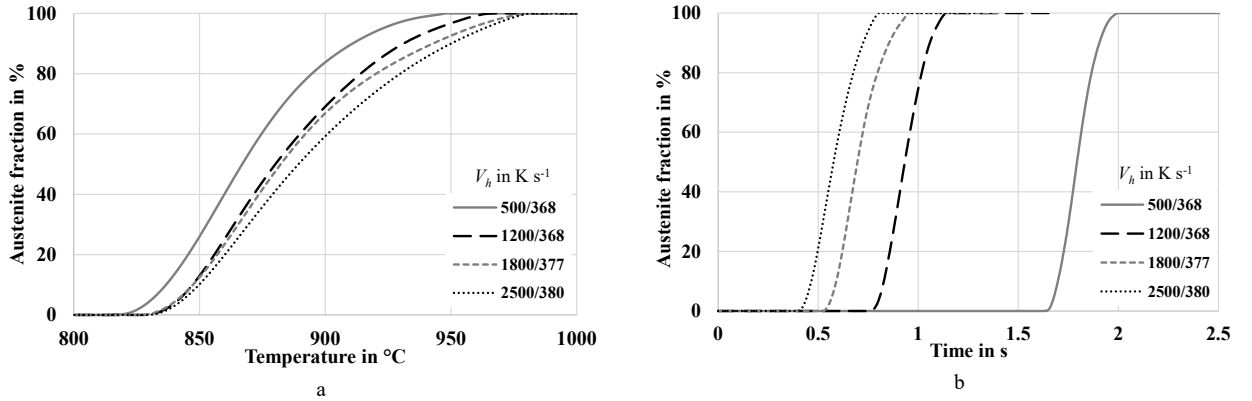

Fig. 5. Austenite formation as function of temperature (a) and heating time (b) for different heating rates (below/above T_c).

Based on the data from Fig. 5, the dependence of the austenite fraction f_A on the heating temperature T and heating time t can be described by an equation valid in the transformation region between A_{c1} and A_{c3} at the investigated heating rates with an adjusted coefficient of multiple determination R_a^2 = 0.985:

$$f_A(T,t) = a + b \cdot \ln t + c \cdot \ln t^2 + d \cdot \ln T + e \cdot \ln T^2 + f \cdot \ln T^3 + g \cdot \ln T^4, \quad (4)$$

and coefficients presented in Table 1.

Table 1. Coefficients of Eq. (4) describing dependence of austenite fraction on heating temperature and time.

a	1105257139.70662	*c*	10.3307719595046	*e*	142773548.847875	*g*	512198.535705521
b	6.00828133211491	*d*	-648711375.932752	*f*	-13964925.8424486		

In order to verify the results of dilatometric investigations, the microstructure of the heat-treated samples was analyzed by optical microscopy. After the inductive heating without holding, the samples were immediately quenched with pressurized nitrogen. According to [16], the critical cooling rate for the steel 22MnB5 amounts to 25 K s^{-1}. Thus, for ensuring a full martensite formation, the samples were quenched with a cooling rate of 30 K s^{-1}. The optical microscopy revealed that all investigated parameters of the heat-treatment resulted in the formation of a completely martensitic microstructure. Hence, a full austenitizing during the inductive heating for each heating rate was achieved. In Fig. 6, the microstructures in the initial state before heating (Fig. 6(a)) as well as in the quenched state (Fig. 6(b)) after heating at 2500/380 K s^{-1} (the most unlikely conditions for full austenitizing) are depicted. The initial state exhibits a typical ferritic-pearlitic microstructure in the initial state, while the quenched sample consists completely of martensite.

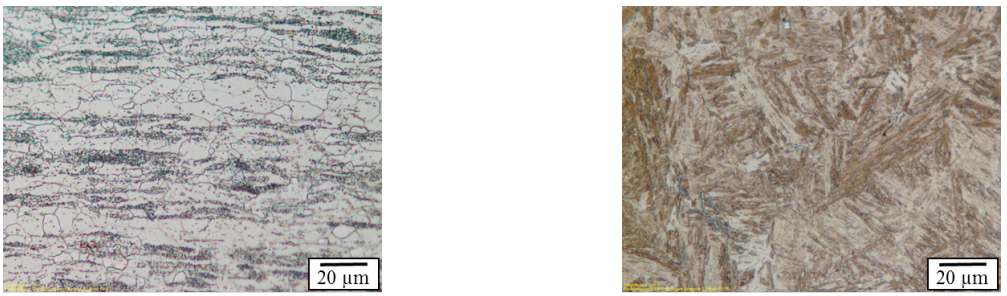

a b

Fig. 6. Optical micrographs of microstructure of steel 22MnB5 (a) in initial as well as quenched state (b) after inductive heating with heating rate of 2500/380 K s^{-1}.

5. Simulation of austenite formation

The obtained data were employed in a simulation of the austenite formation during an inductive heating of a tube from the steel 22MnB5 with dimensions 20 mm × 0.5 mm. The FEM model was generated in ANSYS Workbench and is described in a previous study [17]. In order to determine a real temperature development during the inductive heating in the inline tube forming process, a welded tube with the aforesaid dimensions was heated up in an induction coil with a length of 50 mm at a feed rate of 25 mm/s. The inductor parameters were adjusted for a heating rate of approximately 790/377 K s^{-1}, supposing the heating time of 2 s. Temperature trends were recorded with a thermographic camera, type ThermaCam SC 3000 from FLIR Systems Inc., as well as a thermocouple attached to the internal surface of the tube. The temperature field obtained when the first cross-section left the induction coil was mapped onto the corresponding FEM-mesh nodes (Fig. 7(a)).

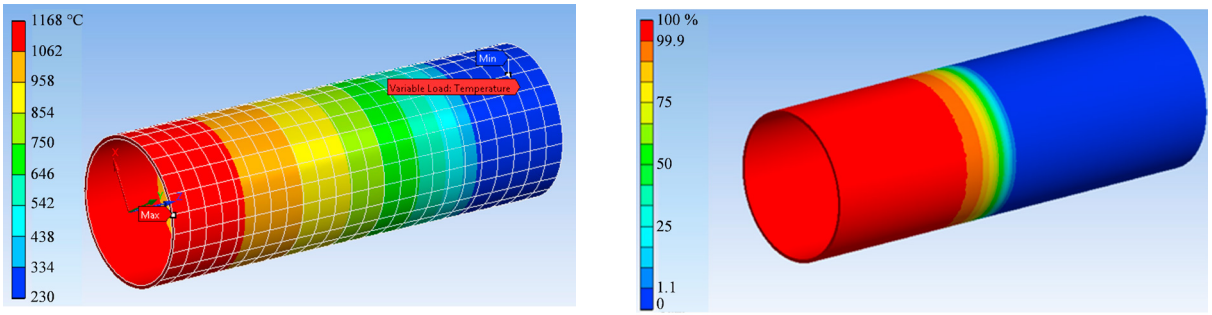

a b

Fig. 7. (a) Temperature field in tube due to inductive heating of 1.25 s at heating rate of 790/377 K s^{-1} mapped in ANSYS Workbench; (b) austenite fraction as function of heating temperature and heating time.

Furthermore, Eq. (4) was applied to determine the austenite fraction in each element. The temperature value was taken from the temperature field and the time was calculated based on a point of ingoing into the induction coil and the given feed rate. The defined values were introduced into Eq. (4) and the austenite fraction in each finite element was determined. The computations were realized using the command snippet and the embedded program language APDL. The obtained austenite fraction is illustrated in Fig. 7(b).

The results of the described simulation model can be used as input data for a subsequent determination of the phase composition of the steel 22MnB5 during cooling and austenite decomposition.

6. Summary

In the present study, the transformation kinetics of the austenite formation due to inductive heating at heating rates in the range from 500 K s^{-1} to 2500 K s^{-1} were investigated. The results can be summarized as follows:

- The target heating rates were valid up to the Curie temperature of the steel. After the loss of the ferromagnetic properties, the heating rates decreased to 368 K s^{-1} - 380 K s^{-1}. The results are of key interest for understanding the heating and transformation kinetics during the inductive heating in the inline process of tube forming.
- Due to the decreased heating rates above the Curie temperature including in the transformation area, the austenite formation occurred similarly for all experiments. However, a shift of the transformation to higher temperatures as a result of increasing heating rates was observed.
- A TTA-diagram for the investigated parameters considering the unstable heating process was suggested. It implies the enlarging of the two-phase region, namely a longer-term transformation of ferrite to austenite. The A_{c1}- (816 - 832 °C) and A_{c3}- (946 - 995 °C) temperatures increased compared to literature describing lower heating rates. A complete austenite formation was expected for all investigated heating parameters and verified by means of optical microscopy.
- A model describing the austenite formation as a function of temperature and time was derived and implemented to simulate the heating process and austenite formation in ANSYS Workbench.

Acknowledgements

The authors thank the German Research Foundation for financial support of the work carried out within the scope of the graduate school's IRTG 1627 "Virtual Materials and Structures and their Validation", subproject C5 "Virtual Design and Manufacturing of Tailored Tubes". Special thanks go to Daniel Rosenbusch from the Institute of Forming Technology and Machines (IFUM) for performing the dilatometric investigations.

References

[1] M. Merklein, M. Johannes, M. Lechner, A. Kuppert, A review on tailored blanks—Production, applications and evaluation, Journal of Materials Processing Technology, 214 (2014) 151–164.

[2] BS EN 10305-2, “Steel tubes for precision applications Welded cold drawn tubes”, (2002).
[3] BS EN 10305-3, “Steel tubes for precision applications Welded cold sized tubes”, (2002).
[4] Y. Chang, C.Y. Wang, K.M. Zhao, H. Dong, J.W. Yan, An introduction to medium-Mn steel: Metallurgy, mechanical properties and warm stamping process, Materials and Design, 94 (2016) 424–432.
[5] G. Halmos, Roll forming handbook, Published by CRC Press, (2006), ISBN 9780824795634.
[6] S. Herbst, K.F. Steinke, H.J. Maier, A. Milenin, F. Nürnberger, Determination of heat transfer coefficients for complex spray cooling arrangements, International Journal of Microstructure and Materials Properties, 11 (2016) 229–246.
[7] M. Spittel, T. Spittel, Steel symbol/number: 22MnB5/1.5528, Warlimont, H. (Hrsg.): SpringerMaterials – The Landolt-Boernstein Database, Springer-Verlag Berlin Heidelberg, (2009), DOI: 10.1007/978-3-540-44760-3_146.
[8] H. Karbasian, A.E. Tekkaya, A review on hot stamping, Journal of Materials Processing Technology, 210 (2010) 2103–2118.
[9] T. Maeno, K. Mori, M. Sakagami, Y. Nakao, Full hardening of products in hot stamping using rapid resistance heating, Proceedings of 5th International Conference on Hot Sheet Metal Forming of High-performance Steel, (2015) 323–330.
[10] A. Guk, A. Kunke, V. Kräusel, D. Landgrebe, Influence of inductive heating on microstructure and material properties in roll forming processes, AIP Conference Proceedings, 1896 (2017), DOI:/10.1063/1.5008107.
[11] T. Tröster, J. Niewel, Inductive heating of blanks and determination of corresponding process windows for press hardening, Report for prohect P 805 / IGF-Nr.16319 N, (2014).
[12] R. Haimbaugh, Practical induction heat treating, second edition, published by ASM International, (2015), ISBN 9781627080897.
[13] R. Kolleck, R. Veit, M. Merklein, J. Lechler, M. Geiger, Investigation on induction heating for hot stamping of boron alloyed steels, CIRP Annals - Manufacturing Technology, 58 (2009) 275–278.
[14] T. Miokovic, J. Schwarzer, V. Schulze, O. Vöhringer, D. Löhe, Description of short time phase transformations during the heating of steels basedon high-rate experimental data, Journal de Physique IV, 120 (2004) 591–598.
[15] J. Kuepferle, J. Wilzer, S. Weber, W. Theisen, Thermo-physical properties of heat-treatable steels in the temperature range relevant for hot-stamping applications, Journal of Material Science, 50 (2015) 2594–2604.
[16] M. Naderi, A.S. Akbari, W. Bleck, The effects of non-isothermal deformation on martensite transformation in 22MnB5 steel, Materials Science and Engineering: A, 487 (2008) 445–455.
[17] I. Hordych, V. Boiarkin, D. Rodman, F. Nürnberger, Manufacturing of tailored tubes with a process integrated heat treatment, AIP Conference Proceedings, 1896 (2017), DOI:/10.1063/1.5008216.